Journal of Neuroimaging in Psychiatry & Neurology

http://dx.doi.org/10.17756/jnpn.2016-002

Research Article

Open Access

^{18}F-AV133 Cerebral VMAT2 Binding Correlated with α-synuclein Spliced Variants in Parkinson's Disease

Rui Gao[1,2], Guangjian Zhang[3], Xueqi Chen[2,4], Savina Reid[2] and Yun Zhou[2*]

[1]Department of Nuclear Medicine, the First Affiliated Hospital of Xian Jiaotong University, Xi'an, Shaanxi, China
[2]The Russell H. Morgan Department of Radiology and Radiological Science, Johns Hopkins University School of Medicine, Baltimore, MD, USA
[3]Department of Surgery, the First Affiliated Hospital of Xian Jiaotong University, Xi'an, Shaanxi, China
[4]Department of Nuclear Medicine, Peking University First Hospital, Beijing, China

[*]Correspondence to:
Yun Zhou, PhD
The Russell H. Morgan Department of Radiology and Radiological Science
Johns Hopkins University School of Medicine
601 N. Caroline Street, JHOC room 3241
Baltimore, MD 21287-0807, USA
Fax: +1 410 955 0696
E-mail: yunzhou@jhmi.edu

Received: October 29, 2015
Accepted: January 08, 2016
Published: January 12, 2016

Citation: Gao R, Zhang G, Chen X, Reid S, Zhou Y. 2016. ^{18}F-AV133 Cerebral VMAT2 Binding Correlated with α-synuclein Spliced Variants in Parkinson's Disease. *J Neuroimaging Psychiatry Neurol* 1(1): 4-9.

Published by United Scientific Group

Abstract

The study was designed to evaluate the connections between genotyping and functional image-based phenotyping in Parkinson's disease (PD). The associations between ^{18}F-AV133 cerebral vesicular monoamine transporter 2 (VMAT2) binding and α-synuclein gene (SNCA) spliced variants were studied within the Parkinson's Progression Markers Initiative study (PPMI) project. ^{18}F-AV133 PET, structural magnetic resonance imaging (MRI), clinical assessments, and α-synuclein isoform data for 22 PD patients and 4 controls were collected from the PPMI project. Eight out of the 22 PD patients undertaken ^{18}F-AV133 PET were presented with SNCA transcript measurements. The ^{18}F-AV133 cerebral standardized uptake value ratio (SUVR) relative to the occipital cortex was calculated as an index of VMAT2 density. The differential expression of 5 SNCA transcript variants (the transcript with boundaries (E3E4), lack exon 5 (E4E6), specifically with a long 3'UTR region (3UTR1 and 3UTR2), and only comprises exons 1-4 (007)) was ascertained by the use of isoform-specific primers and a high-precision Nano String gene expression assay. Region of interest (ROI)- and voxel-wise-based statistical analysis were performed using statistical parametric mapping software (SPM8). In contrast to controls, the highest reduction of ^{18}F-AV133 SUVRs was found in left (contralateral to the predominantly affected side at onset) posterior putamen (54.1%), followed by right posterior putamen (43.2%), left anterior putamen (35.6%), right anterior putamen (27.9%), caudate (22.7%) ($p < 0.01$).The predominantly affected side at onset was right for seven out of the eight PD patients. There were significant correlations between ROI SUVRs and SNCA transcript variants: left anterior putamen with SNCA-007 (Pearson r = 0.85, $p < 0.01$); left anterior putamen with SNCA-E4E6 (r = 0.77, $p = 0.03$); left caudate with SNCA-E3E4 (r = 0.72, $p = 0.04$); and left ventral striatum with SNCA-E3E4 (r = 0.85, $p < 0.01$). Voxel-wise analysis showed that the left sub-lobar and anterior putamen were correlated with SNCA-007, and the left subcallosal gyrus and ventral striatum were significantly correlated with SNCA-E3E4 ($p < 0.001$). The initial results demonstrated a connection between SNCA splice variants in blood and monoaminergic degenerations in PD measured by ^{18}F-AV133 PET.

Keywords

PET, ^{18}F-AV133, Vesicular monoamine transporter 2, Alpha-synuclein isoform, Parkinson's disease

Introduction

Vesicular monoamine transporter 2 (VMAT2) is the protein responsible

for transporting both dopamine and serotonin into synaptic vesicles [1]. [11]C-dihydrotetrabenazine ([11]C-DTBZ) PET has been used for in vivo imaging of cerebral VMAT2, and has proven to be a potential quantitative biomarker for monitoring dopaminergic degeneration in PD [2, 3]. One major limitation of the tracer is its short physical half-life (20 min) for wide use. [18]F-9-fluoropropyl-(+)-dihydrotetrabenazine ([18]F-DTBZ, or [18]F-AV133 hereafter), a recently developed positron emission tomography (PET) tracer forVMAT2 imaging with a half-life of 110 minutes, has shown to be a promising tracer for clinical use for detecting and monitoring the VMAT2 reduction in PD [4-6]. Previous imaging studies demonstrate the feasibility of [18]F-AV-133 to differentiate normal controls from PD subjects [4, 5]. A recent publication clearly indicated the sensitivity of [18]F-AV-133 for detecting monoaminergic terminal reductions in PD patients [5].

Alpha-synuclein, which plays a key role in the development of Lewy body diseases, has been intensely studied over the past decade [7, 8]. Complex splicing events within the α-synuclein gene (SNCA) caused isoforms are known to modify α-synuclein aggregation propensities [9, 10]. The physical, biochemical, and biological properties of alternative SNCA isoforms, therefore, are strongly associated with the pathogenesis of Lewy body diseases [11]. Accumulating evidence suggests that α-synuclein isoforms with different aggregation properties are strongly associated with the progression of PD [11, 12].

Several sensitive, specific and readily available α-synuclein splice variant specific biomarkers for PD were reported [13]. Here, the Parkinson's Progression Markers Initiative study (PPMI) project recruited five related forms of the protein, the transcript with boundaries exon 3 and exon 4 (E3E4), lack exon 5 (E4E6), specifically with a long 3'UTR region (3UTR1 and 3UTR2), and only comprises exons 1-4 (007) to evaluate their potency as biomarkers for PD development (http://www.ppmi-info.org/data). With the aim of depicting the role of these SNCA transcripts in the monoaminergic neuron degeneration in PD, we studied correlations between SNCA transcript levels and cerebral VMAT2 densities measured by [18]F-AV133 PET [4-6].

Materials and Methods

[18]F-AV133 PET, MRI acquisition, and image processing

Available [18]F-AV133 PET scans for 22 PD patients and four normal controls, and structural magnetic resonance imaging (MRI) for each subject in the PPMI project was collected in the study by December 2014. Ten-min (2 × 5min) [18]F-AV133 images acquired at 80.8 (± 2.8 SD) min post tracer injection were used for analysis. The dose of AV-133 used was 222.37 ± 17.02 MBq. Details of the data base have previously been reported [14], and up-to-date information on the study can be obtained from the project webpage (http://www.ppmi-info.org/data).

All PET and MRI images were processed using Statistical Parametric Mapping software (SPM8, Wellcome Department of Imaging Neuroscience, London, United Kingdom) and MATLAB (The MathWorks Inc.). To minimize motion effects during PET scan, the [18]F-AV133 images with two frames were first aligned to generate mean images. All the aligned 10-min [18]F-AV133 PET mean images were then co registered to MRI images. The MRI images were normalized to standard Montreal Neurologic Institute (MNI) space using SPM8 [15] with a high resolution MRI template provided by VBM8 toolbox [16]. The transformation parameters determined by MRI spatial normalization were then applied to the co registered PET images for PET spatial normalization. A total of 34 regions of interest (ROIs) including the cortex, striatum, and sub-striatal regions were manually drawn on the MRI template using PMOD software (PMOD Technologies Ltd., Zürich, Switzerland) in standard MNI space. The sub-striatal regions used in the study were the ventral striatum, caudate, anterior putamen (pre-commissural dorsal putamen), and posterior putamen (post-commissural putamen) [17, 18]. The occipital cortex was used as reference tissue to calculate the standardized uptake value ratio (SUVR) of [18]F-AV133 binding (http://www.ppmi-info.org/: AV-133 PET Image Processing Methods for Calculation of Striatal Binding Ratio), where the SUVR is a quantitative measurement of VMAT2 density in brain tissues. SUVR images were calculated as PET (images)/PET (occipital) in the standard space (image volume: 121 × 145 × 121, voxel size: 1.5 × 1.5 × 1.5 mm in x, y, z). ROI SUVRs were then obtained by applying ROIs to SUVR images. A 3D spatial Gaussian filter of 8 mm full width at half maximum in x, y, z direction was applied to SUVR images for voxel-wise statistical analysis using SPM8.

SNCA transcript analysis

Eight out of the 22 PD patients who underwent [18]F-AV133 PET scanning also presented SNCA transcript measurements. The 8 PDs were comprehensively assessed for clinical characteristics, imaging manifestations, and blood indicators as described in the PPMI biologics manual (http://www.ppmi-info.org/).

The biospecimens processing was performed in a standardized manner. Venous blood was collected briefly from each subject in PAX gene (Qiagen, Valencia CA) tubes, incubated at room temperature for 24 hours, and frozen and shipped on dry ice to Coriell. RNA was extracted following the PAX gene procedure. RNA quality was determined by using the RNA Integrity Number package. Only RNAs meeting three stringent Q/C parameters will be included in the analysis. Probes for the target and control RNAs were multiplexed and assayed according to the manufacturer's protocol on the n Counter Digital Analyzer. Five SNCA probes were used to target the boundaries of exon 3 and exon 4 (E3E4-SNCA), transcripts specifically with a long 3'UTR region (3UTR-1- and 3UTR2-SNCA), transcripts that skip exon 5 (E4E6-SNCA), and the rare short SNCA-007 transcript isoforms (Ensembl ID ENST00000506691) that comprises exons 1-4 (www.ensembl.org). Transcript counts were assayed in human blood in a high-precision NanoString gene expression assay that directly measures RNA counts in total RNA without bias from reverse transcription into cDNA. No template (negative) controls containing water substituted for template were included. To control for plate-to-plate variation and drift, equal amounts of RNA derived

from Human Universal Reference RNA were spotted at the beginning, end, and throughout the entire experiment.

Statistical analysis

ROI-based analyses were performed with Statistical Package for the Social Sciences (SPSS) statistics (version 21; SPSS, Inc., Chicago, IL). Comparisons of ROI SUVRs between Parkinson's disease and healthy controls were tested with independent t tests. Based on the unified Parkinson disease rating scale (UPDRS) Part III (Motor scale) [19], PD patients were sub-grouped into severely disabled (SD-PD, Motor Scale > 32) and mild-to-moderately disabled (MD-PD, Motor Scale ≤ 32).

The relationships between the SNCA splice variants and ROI SUVRs were explored by Pearson's correlations. ROI-based analysis is a hypothesis driven approach with PET measurement of high signal to noise ratio, but limited to predefined ROIs. Complementary to ROI-based analysis, voxel-wise statistical analysis was performed using SPM8 in the study. Statistical parametric maps were obtained for each SNCA splice variant by linear regression between SUVR images and SNCA transcript counts. For the relatively higher noise levels of voxel-wise SUVR measurements, results of linear regressions were reported at a p-value < 0.001 for clusters > 50 voxels. To study the spatial and temporal changes of ^{18}F-AV133 VMAT2 binding in PD progression, the images of the PD patients were reoriented so that the striatum contralateral to the symptomatic side was always on the left of the brain [20].

Table 1: Demographics and clinical assessments of subjects with ^{18}F-AV133 PET.

	PD (n = 22)		HC (n = 4)	*P*
	MD-PD (n = 17)	SD-PD (n = 5)		
Age (years)	62.18 ± 11.02	66.60 ± 6.89	63.37 ± 11.77	> 0.1
Gender (male: female)	14:3	4:1	3:1	> 0.5
Disease duration (months)	17.89 ± 4.85	19.36 ± 6.38	/	> 0.1
UPDRS total score	29.0 ± 8.98	53.2 0 ± 4.66	2.50 ± 2.08	< 0.01*§
Hoehn and Yahr stage	1.42 ± 0.49	2.0	/	< 0.01§
MoCA	26.12 ± 3.18	25.2 ± 2.14	27.75 ± 0.96	> 0.05
Side predominantly affected at onset (R: L)	10:7	4:1	/	> 0.1

Data are presented as mean ± SD; HC, elderly health control; PD, Parkinson's disease; MD-PD, mild to moderate disabled PD; SD-PD, severely disabled PD; UPDRS, unified Parkinson disease rating scale; MoCA, Montreal cognitive assessment, R, right; L, left.; *, comparison between PD and HC; §, comparison between SD-PD and MD-PD.

Results

Demographics, statistics of clinical assessments, ^{18}F-AV133 ROI SUVRs and SNCA transcripts

Demographics and simple statistics of 22 PD patients and 4 controls that had ^{18}F-AV133 PET scans were summarized in Table 1. The mean age of these patients was 64.51 years, which was not significantly different from the mean age (63.37 years) of health controls (p > 0.5). The disease duration was comparable between MD-PD (17.89 ± 4.85 months, n = 17) and SD-PD group (19.36 ± 6.38, n = 5). There was also no statistical difference in MoCA between PD patients and the control group. Among these 22 patients with PET data, the statistics for the 8 PD patients who had SNCA transcript values were listed in Table 2. The age, MoCA score, Motor scales, and ROI SUVRs of the 8 patients were not significantly different from those in the MD-PD or whole PD group.

Table 2: Statistics of the 8 PD patients with both SNCA transcripts and ^{18}F-AV133 PET.

		PD patients (n = 8)
Baseline information	Age (years)	62.38 ± 6.82
	Sex (M: F)	6:2
	Handedness (R: L: Mi)	6:1:1
PD features and medications	UPDRS Part III (Motor Scale)	25.13 ± 8.52
	Hoehn and Yahr stage	1.63 ± 0.48
	MoCA score	25.25 ± 3.80
	Resting tremor (P: N)	7:1
	Rigidity (P: N)	7:1
	Bradykinesia (P: N)	7:1
	Postural instability (P: N)	0:8
	Side predominantly affected at onset (R: L)	7:1
	L-dopa medication (P: N)	3:5
SNCA transcript variants count	SNCA-3UTR-1	1803.63 ± 607.80
	SNCA-3UTR-2	526.75 ± 185.17
	SNCA-007	29.38 ± 37.50
	SNCA-E3E4	12441.88 ± 5536.38
	SNCA-E4E6	1970.12 ± 633.69

Data are presented as mean ± SD; PD, Parkinson's disease; UPDRS, unified Parkinson disease rating scale; MoCA, Montreal cognitive assessment; M, Male; F, Female; R, Right; L, Left; Mi, Mixed; P, Positive; N, Negative; SNCA, α-synuclein gene; SNCA-E3E4, the transcript with boundaries exon 3 and exon 4; SNCA-E4E6, the transcript lack exon 5; SNCA-3UTR-1 and 2, the transcript specifically with a long 3'UTR region; SNCA-007, the transcript only comprises exons 1-4.

The simple statistics of ROI SUVRs of ^{18}F-AV133 binding in PD patients were illustrated in Figure 1. There were remarkable reduced SUVRs in the PD group (n = 22) in striatal sub-regions as compared to healthy controls (n = 4). The highest reduction of ^{18}F-AV133 SUVRs was found in left posterior putamen (54.1%); followed by right posterior putamen (43.2%), left anterior putamen (35.6%), right anterior putamen (27.9%), caudate (22.7%) (p < 0.01), and non-significant reductions in substantia nigra (12.4%, p = 0.09) and ventral striatum (7.1%, p = 0.42).Although there were no significant differences in SUVRs between the MD-PD group (n = 17) and the SD-PD group (n = 5), a trend of reduced SUVR was found in the right anterior putamen, caudate, ventral striatum, and substantia nigra (p, 0.10 - 0.40), and an increased MoCA score in SD-PD (25.20 ± 2.14 vs. 26.12 ± 3.18, p = 0.57). It is expected that these differences between the MD-PD and SD-PD group will attain statistical significance with a sample size comparable to the ones reported

by Hsiao et al., especially for the SD-PD group [5]. It is worth to note that the left is referred to the side contralateral to the side predominantly affected at onset.

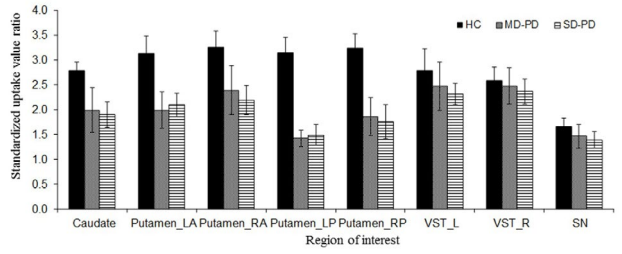

Figure 1: The [18]F-AV133 standardized uptake value ratios (SUVRs) (mean ± SD) of striatal sub-regions in five severely disabled (SD-PD, Motor Scale > 32) and 17 mild-to-moderately disabled (MD-PD, Motor Scale ≤32) PD patients, and 4 elderly health controls (HC). Note that the left is the side contralateral to the predominantly affected side at onset in PD patient. VST, ventral striatum; SN, substantia nigra; L, left; R, right; LA, left anterior; LP, left posterior; RA, right anterior; RP, right posterior.

Correlations between SNCA transcripts counts and cerebral [18]F-AV133 SUVRs in Parkinson's disease

The short SNCA-007 transcript and SNCA-E4E6 transcript had significant positive correlations with and the left anterior putamen SUVRs (Pearson r = 0.85, $p < 0.01$; and r = 0.77, $p = 0.03$). The SNCA-E3E4 was positively correlated with SUVRs of the left caudate and ventral striatum (Pearson r = 0.72, $p = 0.04$; and r = 0.85, $p < 0.01$, Figure 2. A representative SUVR image from a typical PD patient with higher SNCA-007/-E4E6/-E3E4 levels had higher SUVRs in the striatum and better UPDRS motor scale/MoCA score as compared to a patient of low SNCA-007/-E4E6/-E3E4 counts (Figure 3). Note there were no significant correlations between the transcripts SNCA-3'UTR-1 and SNCA-3'UTR-2 counts and ROI [18]F-AV133 SUVRs.

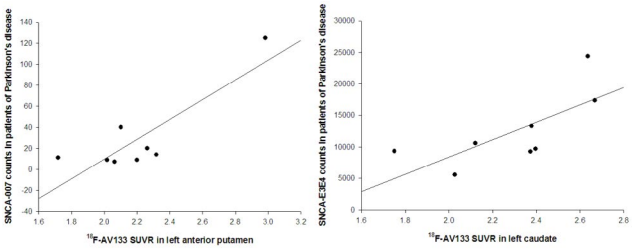

Figure 2: Linear correlations between SNCA transcript variants and [18]F-AV133 ROI SUVRs in PD patients (n = 8). The correlations were significant with $p < 0.05$.

Results from voxel-wise statistical analysis showed that a single large cluster of 653 voxels (peak $T = 9.92$ at -33 mm, 12 mm, -8 mm in x, y, z), mainly involving the left sub-lobar and left anterior putamen, was positively correlated with SNCA-007 counts (Figure 4A). SPM8 analysis also detected positive correlations between SNCA-E3E4 counts and a cluster of 194 voxels (peak $T = 8.12$ at - 6 mm, - 17 mm, -14 mm in x, y, z), mainly including voxels located in the left subcallosal gyrus and ventral striatum (Figure 4B).

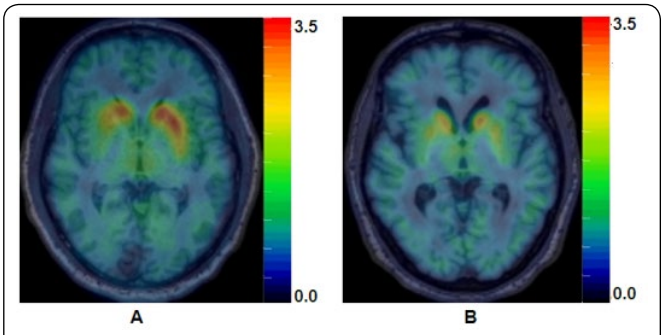

Figure 3: Representative [18]F-AV133 SUVR images of two PD patients with different SNCA transcript levels. **A:** a 60-y-old male with SNCA-007/-E4E6/-E3E4 of 125/2810/17346 counts; **B:** a 65-y-old male with SNCA-007/-E4E6/-E3E4 of 11/1005/5562 counts. The UPDRS motor scale/MoCA score for patient A and B were 16/27 and 35/22, respectively. [18]F-AV133 ROI SUVRs for patient A and B were: caudate, 2.21 and 1.66; left putamen, 2.72 and 1.61; right putamen, 1.93 and 1.63; ventral striatum, 2.43 and 2.31; raphe nuclei, 1.81 and 1.67; and substantia nigra, 1.63 and 1.14, respectively.

Discussion

It has been reported that PARK proteins are associated with familial forms of Parkinson's disease over the past decade. The mutations in genes clustered in the PARK loci, including PARK1 (α-synuclein, SNCA), PARK2 (parkin), PARK5 (UCH-L1), PARK6 (PINK1), PARK7 (DJ-1), PARK8 (LRRK2) and PARK9 (ATP13A2), are linked to the disease [21]. The aggregations of a-synuclein are considered one of the central factors in the pathophysiology of PD [8,11]. In addition to a number of post-translational modifications, including phosphorylation, nitration, cleavage, and ubiquitination [22], four α-synuclein spliced mRNA transcripts have been reported till now: SNCA140 (the full-length isoform), SNCA126 (lack exon 3), SNCA112 (lack exon 5), and SNCA98 (lack exon 3 and 5) [10-12]. Specific RNA transcript isoforms with an extended 3′ untranslated region were also reported to be linked to pathological processes [23]. Besides the above mentioned splice variants, the PPMI recruited five related forms of the SNCA transcripts to evaluate their potency as biomarkers for PD development (http://www.ppmi-info.org/data). As the monoaminergic terminal reductions evaluated by [18]F-AV-133 image has been taken as an objective marker for PD development [2-6], the current study evaluated the association between SNCA splices variant biomarkers and cerebral [18]F-AV-133 SUVRs in PD. ROI-based and voxel-wise analysis showed there were significant positive correlations between [18]F-AV133 SUVRs of the ventral striatum, caudate, and anterior putamen/sub-lobar, and α-synuclein transcript levels of SNCA-007 and SNCA-E3E4 (Figure 2 and 4). These strong correlations suggest a possibility of using these SNCA transcripts as biomarkers for monoaminergic neuron degenerations in PD. A report from Zaltieri et al and Wang et al provides support to our findings. Their study proved the involvement of α-synuclein in synaptic transmission in knock-out mice and suggested that that α-synuclein may regulate the size of presynaptic vesicular pools [24, 25]. Consequently, it can be suggested that these α-synuclein isoforms play a role in neurotransmission or in the organization and regulation of pre-synaptic VMAT2 vesicles.

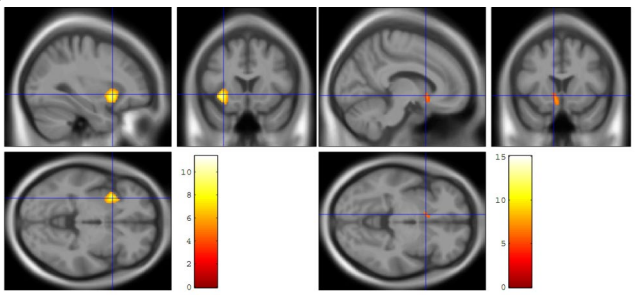

Figure 4: Statistical t map on MRI template. A: voxel SUVRs in the cluster (left sub-lobar and anterior putamen) were correlated with SNCA-007 counts; and B: voxel SUVRs in the cluster (left subcallosal gyrus and ventral striatum) were correlated with SNCA-E3E4counts. $p < 0.001$ and cluster > 50 voxels were selected in SPM analysis.

In line with previous reports indicating presynaptic α-synuclein aggregation is involved in synaptic function [25], the current study showed a significant positive correlation between α-synuclein transcripts and cerebral [18]F-AV133 SUVRs. While the biological and pathological significance of the different α-synuclein splicing variants remains unknown, these isoforms have been associated with intracellular aggregations [26-29]. Though accelerated fibrillogenesis and enhanced aggregation was expected with the deletion of the functional domains [10, 29], the alternative isoforms actually aggregate less than the canonical isoform SNCA140 [12]. The interruption of the domain responsible for protein–membrane interaction at the protein N-terminus even makes SNCA 126 an aggregation-preventing isoform [28]. In this way, we surmise that transcripts SNCA-007 and SNCA–E3E4, which correlated positively with the monoaminergic neuron function, were neuron protective isoforms. Further studies are needed to clarify the mechanism underlie our findings.

Our study found a significant correlation between α-synuclein transcripts and monoaminergic neuronal function in the anterior putamen, caudate, and ventral striatum in PD patients. These brain regions are known for their crucial role in regulating dopaminergic activity associated with cognitive function in PD [30-32]. Accumulating evidence suggests that dopamine depletion spreading to the ventral striatum disrupts corticostriatal communication, and the relationship between striatal and cortex dopamine should be considered as important contributors to cognitive decline [32, 33]. As α-synuclein has long been suggested to be involved in cognitive decline of Alzheimer's disease (AD) and PD [34, 35], our results shed some light on the way to explain the role of α-synuclein in cognitive decline in PD.

Since VMAT2 is a neuro transporter not only for dopamine, but also for serotonin, norepinephrine, histamine, and GABA.The reductions in VMAT2 PET measurements could reflect the brain dysfunction in PD patients.A recent study reported that there werecorrelations between cognitive status and striatal [18]F-AV133 binding in Dementia with Lewy Bodies (DLB) [36]. Although we did not find any close correlations between regional SUVRs of [18]F-AV133 and cognitive assessments in our PD patients (including HVLT-R, BJLO, LNS, SDMT, semantic fluency, and the phonemic fluency test, n = 22), a convergent decline of striatal VMAT2 density and MoCA scores was found in severely disabled patients. Not all patients with Parkinson's disease in our study had measurable cognitive impairment (mean MoCA score 25.5). Thus, it is possible that more pronounced changes and stronger associations with cognition might be detected in a large PD population with established cognitive deficit in the ongoing project.

In conclusion, this pilot study provided the first evidence of a strong linear correlation between SNCA splice variant markers and cerebral VMAT2 densities measured by [18]F-AV133 SUVRs in PD. The results indicate that α-synuclein splicing may represent an important regulatory and/or functional role during PD development. Considering the high heterogeneity in PD development, we realized one main limitation of the study is that the SNCA expression and VMAT2 correlation study was based on only eight patients. This reduced sample size could explain the lack of consistence between ROI-based results and results from voxel-wise analysis. As the PPMI is ongoing project, we will continue to study the associations between SNCA spliced variants and cerebral VMAT2 densities with larger population.

Acknowledgements

Data used in the preparation of this article were obtained from the PPMI database (www.ppmi-info.org/data). For up-to-date information on the study, visit www.ppmi-info.org. PPMI-a public-private partnership-is funded by the Michael J. Fox Foundation for Parkinson's Research and funding partners, including AbbVie, Avid Radiopharmaceuticals, Biogen Idec, Bristol-Myers Squibb, Covance, GE Healthcare, Genentech, GlaxoSmithKline, Lilly, Lundbeck, Merck, Meso Scale Discovery, Pfizer Inc., Piramal Imaging, Roche, Servier, and UCB.

References

1. Guillot TS, Miller GW. 2009. Protective actions of the vesicular monoamine transporter 2 (VMAT2) in monoaminergic neurons. *Mol Neurobiol* 39(2): 149-170. doi: 10.1007/s12035-009-8059-y
2. Koeppe RA, Frey KA, Kume A, Albin R, Kilbourn MR, et al. 1997. Equilibrium versus compartmental analysis for assessment of the vesicular monoamine transporter using (+)-alpha-[11C] dihydrotetrabenazine (DTBZ) and positron emission tomography. *J Cereb Blood Flow Metab* 17(9): 919-931. doi: 10.1097/00004647-199709000-00001
3. Koeppe RA, Frey KA, Kuhl DE, Kilbourn MR. 1999. Assessment of extrastriatal vesicular monoamine transporter binding site density using stereoisomers of [11C]dihydrotetrabenazine. *J Cereb Blood Flow Metab* 19(12): 1376-1384. doi: 10.1097/00004647-199912000-00011
4. Okamura N, Villemagne VL, Drago J, Pejoska S, Dhamija RK, et al. 2010. In vivo measurement of vesicular monoamine transporter type 2 density in Parkinson disease with (18)F-AV-133. *J Nucl Med* 51(2): 223-228. doi: 10.2967/jnumed.109.070094
5. Hsiao IT, Weng YH, Lin WY, Hsieh CJ, Wey SP, et al. 2014. Comparison of 99mTc-TRODAT-1 SPECT and [18]F-AV-133 PET imaging in healthy controls and Parkinson's disease patients. *Nucl Med Biol* 41(4): 322-329. doi: 10.1016/j.nucmedbio.2013.12.017
6. Chao KT, Tsao HH, Weng YH, Hsiao IT, Hsieh CJ, et al. 2012. Quantitative analysis of binding sites for 9-fluoropropyl-(+)-dihydrotetrabenazine ([18]F] AV-133) in a MPTP-lesioned PD mouse model. *Synapse* 66(9): 823-831. doi: 10.1002/syn.21572
7. Norris EH, Giasson BI, Lee VM. 2004. Alpha-synuclein: normal

function and role in neurodegenerative diseases. *Curr Top Dev Biol* 60: 17-54. doi: 10.1016/S0070-2153(04)60002-0

8. Spillantini MG, Schmidt ML, Lee VM, Trojanowski JQ, Jakes R, et al. 1997. Alpha-synuclein in Lewy bodies. *Nature* 388 (6645): 839-840.
9. Beyer K, Lao JI, Carrato C, Mate JL, Lopez D, et al. 2004. Differential expression of alpha-synuclein isoforms in dementia with Lewy bodies. *Neuropathol Appl Neurobiol* 30(6): 601-607. doi: 10.1111/j.1365-2990.2004.00572.x
10. Beyer K. 2006. Alpha-synuclein structure, posttranslational modification and alternative splicing as aggregation enhancers. *Acta Neuropathol* 112(3): 237-251. doi: 10.1007/s00401-006-0104-6
11. McLean JR, Hallett PJ, Cooper O, Stanley M, Isacson O. 2012. Transcript expression levels of full-length alpha-synuclein and its three alternatively spliced variants in Parkinson's disease brain regions and in a transgenic mouse model of alpha-synuclein over expression. *Mol Cell Neurosci* 49(2): 230-239. doi: 10.1016/j.mcn.2011.11.006
12. Bungeroth M, Appenzeller S, Regulin A, Völker W, Lorenzen I, et al. 2014. Differential aggregation properties of alpha-synuclein isoforms. *Neurobiol Aging* 35(8): 1913-1919. doi: 10.1016/j.neurobiolaging.2014.02.009
13. Cardo LF, Coto E, de Mena L, Ribacoba R, Mata IF, et al. 2014. Alpha-synuclein transcript isoforms in three different brain regions from Parkinson's disease and healthy subjects in relation to the SNCA rs356165/rs11931074 polymorphisms. *Neurosci Lett* 562: 45-49. doi: 10.1016/j.neulet.2014.01.009
14. Lebedev AV, Westman E, Simmons A, Lebedeva A, Siepel FJ, et al. 2014. Large-scale resting state network correlates of cognitive impairment in Parkinson's disease and related dopaminergic deficits. *Front Syst Neurosci* 8: 45. doi: 10.3389/fnsys.2014.00045
15. Ashburner J, Friston KJ. 2005. Unified segmentation. *Neuroimage* 26(3): 839-851. doi: 10.1016/j.neuroimage.2005.02.018
16. Gaser C. 2014. Voxel based morphometry extension to SPM8.
17. Martinez D, Slifstein M, Broft A, Mawlawi O, Hwang DR, et al. 2003. Imaging human mesolimbic dopamine transmission with positron emission tomography. Part II: amphetamine-induced dopamine release in the functional subdivisions of the striatum. *J Cereb Blood Flow Metab* 23(3): 285-300. doi: 10.1097/01.WCB.0000048520.34839.1A
18. Mawlawi O, Martinez D, Slifstein M, Broft A, Chatterjee R, et al. 2001. Imaging human mesolimbic dopamine transmission with positron emission tomography: I. Accuracy and precision of D(2) receptor parameter measurements in ventral striatum. *J Cereb Blood Flow Metab* 21(9): 1034-1057. doi: 10.1097/00004647-200109000-00002
19. Martínez-Martín P, Rodríguez-Blázquez C, Mario Alvarez, Arakaki T, Arillo VC, et al. 2015. Parkinson's disease severity levels and MDS-Unified Parkinson's Disease Rating Scale. *Parkinsonism Relat Disord* 21(1): 50-54. doi: 10.1016/j.parkreldis.2014.10.026
20. Wang J, Zuo CT, Jiang YP, Guan YH, Chen ZP, et al. 2007. [18]F-FP-CIT PET imaging and SPM analysis of dopamine transporters in Parkinson's disease in various Hoehn & Yahr stages. *J Neurol* 254(2): 185-190. doi: 10.1007/s00415-006-0322-9
21. Schiesling C, Kieper N, Seidel K, Krüger R. 2008. Familial Parkinson's disease--genetics, clinical phenotype and neuropathology in relation to the common sporadic form of the disease. *Neuropathol Appl Neurobiol* 34(3): 255-271. doi: 10.1111/j.1365-2990.2008.00952.x
22. Oueslati A, Fournier M, Lashuel HA. 2010. Role of post-translational modifications in modulating the structure, function and toxicity of alpha-synuclein: implications for Parkinson's disease pathogenesis and therapies. *Prog Brain Re* 183: 115-145. doi: 10.1016/S0079-6123(10)83007-9
23. Rhinn H, Qiang L, Yamashita T, Rhee D, Zolin A, et al. 2012. α-Synuclein transcript alternative 3′UTR usage as a convergent mechanism in Parkinson's disease pathology. *Nat Commun* 3: 1084.
24. Zaltieri M, Grigoletto J, Longhena F, Navarria L, Favero G, et al. 2015. α-synuclein and synapsin III cooperatively regulate synaptic function in dopamine neurons. *J Cell Sci* 128: 2231-2243. doi: 10.1242/jcs.157867
25. Wang L, Das U, Scott DA, Tang Y, McLean PJ, et al. 2014. α-synuclein multimers cluster synaptic vesicles and attenuate recycling. *Curr Biol* 24(19): 2319-2326. doi: 10.1016/j.cub.2014.08.027
26. Kalivendi SV, Yedlapudi D, Hillard CJ, Kalyanaraman B. 2010. Oxidants induce alternative splicing of alpha-synuclein: Implications for Parkinson's disease. *Free Radic Biol Med* 48(3): 77-83. doi: 10.1016/j.freeradbiomed.2009.10.045
27. McLean PJ, Hyman BT. 2002. An alternatively spliced form of rodent alpha-synuclein forms intracellular inclusions in vitro: role of the carboxy-terminus in alpha-synuclein aggregation. *Neurosci Lett* 323(3): 219-223. doi: 10.1016/S0304-3940(02)00154-4
28. Beyer K, Humbert J, Ferrer A, Lao JI, Carrato C, et al. 2006. Low a-synuclein 126 mRNA levels in dementia with Lewy bodies and Alzheimer disease. *Neuro Report* 17: 1327-1330. doi: 10.1097/01.wnr.0000224773.66904.e7
29. Beyer K, Ariza A. 2013. α-Synuclein posttranslational modification and alternative splicing as a trigger for neurodegeneration. *Mol Neurobiol* 47(2): 509-524. doi: 10.1007/s12035-012-8330-5
30. Suhara T, Yasuno F, Sudo Y, Yamamoto M, Inoue M, et al. 2001. Dopamine D2 receptors in the insular cortex and the personality trait of novelty seeking. *Neuroimage* 13(5): 891-895. doi: 10.1006/nimg.2001.0761
31. Kaasinen V, Aalto S, Någren K, Rinne JO. 2004. Insular dopamine D2 receptors and novelty seeking personality in Parkinson's disease. *Mov Disord* 19(11): 1348-1351. doi: 10.1002/mds.20191
32. Christopher L, Marras C, Duff-Canning S, Koshimori Y, Chen R, et al. 2014. Combined insular and striatal dopamine dysfunction are associated with executive deficits in Parkinson's disease with mild cognitive impairment. *Brain* 137: 565-575. doi: 10.1093/brain/awt337
33. Cools R, Ivry RB, D'Esposito M. 2006. The human striatum is necessary for responding to changes in stimulus relevance. *J Cogn Neurosci* 18(12): 1973-1983. doi: 10.1162/jocn.2006.18.12.1973
34. Clinton LK, Blurton-Jones M, Myczek K, Trojanowski JQ, LaFerla FM. 2010. Synergistic Interactions between Abeta, tau, and alpha-synuclein: acceleration of neuropathology and cognitive decline. *J Neurosci* 30(21): 7281-7289. doi: 10.1523/JNEUROSCI.0490-10.2010
35. Korff A, Liu C, Ginghina C, Shi M, Zhang J, et al. 2013. α-Synuclein in cerebrospinal fluid of Alzheimer's disease and mild cognitive impairment. *J Alzheimers Dis* 36: 679-688. doi: 10.3233/JAD-130458
36. Siderowf A, Pontecorvo MJ, Shill HA, Mintun MA, Arora A, et al. 2014. PET imaging of amyloid with Florbetapir F 18 and PET imaging of dopamine degeneration with [18]F-AV-133 (florbenazine) in patients with Alzheimer's disease and Lewy body disorders. *BMC Neurol* 14: 79. doi: 10.1186/1471-2377-14-79